Author's final submitted manuscript
**Published as** Rapid Commun. Mass Spectrom., vol. 15, pp. 1422-1426 (2001)
DOI: 10.1002/rcm.380
http://onlinelibrary.wiley.com/doi/10.1002/rcm.380/abstract

# Two-photon ionization thresholds of MALDI matrix clusters

Qiong Lin and Richard Knochenmuss*
Laboratorium für Organische Chemie
Universitätsstr. 16
Swiss Federal Institute of Technology Zurich,
CH-8092 Zürich, Switzerland

**Abstract:**
Direct two-photon ionization of the matrix has been considered a likely primary ionization mechanism in matrix-enhanced laser desorption/ionization (MALDI) mass spectrometry. This mechanism requires that the vertical ionization threshold of matrix materials be below twice the laser photon energy. Because dimers and larger aggregates may be numerous in the early stages of the MALDI plume expansion, their ionization thresholds are important as well. We have used two-color two-photon ionization to determine the ionization thresholds of jet cooled clusters of an important matrix, 2,5-dihydroxy benzoic acid (DHB), and mixed clusters with the thermal decomposition product of DHB, hydroquinone. The thresholds of the clusters were reduced by only a few tenths of an eV compared to the monomers, to an apparent limit of 7.82 eV for pure DHB clusters. None of the investigated clusters can be directly ionized by two nitrogen laser photons (7.36 eV), and the ionization efficiency at the thresholds is low.

* Author for correspondence
tel: ++41 1 632 3875
fax: ++41 1 632 1292
email:knochenmuss@org.chem.ethz.ch

**Introduction**

Matrix assisted laser desorption / ionization (MALDI) mass spectrometry is a relatively recent method,(1) yet has become one of the most important techniques for the analysis of large biomolecules and synthetic polymers.(2,3) It has been developed in a largely empirical manner, and numerous questions remain regarding the generation of both matrix and analyte ions.(4,5)

In positive-ion mode, radical, protonated and alkali-cationized matrix species are frequently observed. Bio-analytes are frequently protonated, synthetic polymers more commonly form metal adduct ions.(6) The ions observed in the mass spectrum are the products of secondary reactions in the expanding plume,(4) and not necessarily reflective of the primary mechanisms leading to the first ions.

MALDI is typically performed with ultraviolet (UV) lasers, and many matrices are derivatized aromatic molecules, so an obvious candidate mechanism is direct photoionization of matrix molecules. Such models figure prominently in the range of possibilities discussed in the literature.(5,7-9) Unfortunately, little data has been available by which such models can be tested or evaluated. To fill this gap, we have begun investigations of the photo physical and photochemical properties of MALDI matrices. Using molecular beam techniques, free matrix molecules and small clusters can be investigated in detail using laser spectroscopy. This approach decouples the desorption and ionization steps, which in MALDI are intertwined. It also avoids in-plume secondary reactions that can significantly change the ion distribution.(4)

Initial results for 2,5 dihydroxy benzoic acid (DHB) have been presented.(10) Free DHB was found to have a sharp two-photon ionization threshold at 8.0475 eV. This is not accessible with two 337 nm nitrogen laser photons (7.36 eV), and rules out a direct single molecule photoionization mechanism for this matrix. However, both experiment and theory suggest that not only single molecules but aggregates and clusters must be considered in MALDI models(11,12). Particles emitted in desorption events have been collected and observed by microscopy,(13) and molecular dynamics simulations of desorption predict large quantities of clusters early in the desorption event.(14) Recent picosecond two-pulse MALDI studies also support this; ionization is most efficient about 2 ns after desorption has begun, when clusters should be prevalent.(15) Since the IPs of clusters are normally lower than those of free molecules due to delocalization effects, their presence could potentially open the two-photon ionization channel. The present work attempts to address this question by measurement of IPs of matrix clusters and clusters of matrix with typical thermal

decomposition products that exist in the MALDI plume.

**Experimental**

A detailed description of the experiment setup can be found elsewhere.(10) The matrix 2,5-dihydroxy benzoic acid (DHB) was purchased from Fluka, and purified by recrystallization before use. It was heated in a pulsed nozzle to temperatures between 170¡ and 180¡C to generate suitable vapor pressures of a few mbar. Neon at 1-2 bar was passed over the matrix and the resulting mixture was expanded into the vacuum through a 400 $\mu$m diameter nozzle. Due to adiabatic expansion cooling, very low internal temperatures are reached, enabling high resolution spectroscopy and more precise ionization threshold determination. By changing the expansion conditions, clusters with various size distributions can be formed. Here, these clusters consisted of up to 10 molecules.

The free matrix molecules and clusters were ionized by via resonance-enhanced two-photon ionization. Two frequency-doubled Lambda Physik dye lasers, pumped by one Continuum Nd:YAG laser, were used to create two independently tunable UV laser beams. The UV pulse energies were typically 30-70 $\mu$J in a pulse of about 5 ns. The laser beams crossed the molecular beam in the acceleration region of a linear 1 m time-of-flight (TOF) mass spectrometer. The 144 V/cm accelerating field reduces the apparent ionization thresholds compared to the field-free values by approximately 0.009 eV.(10) For the clusters studied here, this is less than the uncertainties due to other causes.

The first step was to locate the first electronic absorption band of the molecule or cluster in question. One laser was fixed at a wavelength short enough to ionize the molecule from its first excited state. The other laser was scanned. When this laser became resonant with a ground-to-first excited state transition, ions were generated by subsequent absorption of the fixed-wavelength laser beam. Since detection was mass-selective, the absorption spectrum of each molecule or cluster could be independently measured in one experiment. This technique is known as 2-color resonant two-photon ionization (R2PI) spectroscopy.

After determining the absorption spectrum of each species, the two-photon ionization threshold was measured by scanning the ionization laser. One laser was fixed on a resonant absorption, typically at or near the $S_1$ -> $S_0$ electronic origin band, to get a significant population of molecules or clusters in the first electronically excited state. This absorption was chosen to minimize overlap with other species

present. If this was not unambiguously possible, the expansion conditions could be adjusted to change the relative amounts of different clusters. The differences then clearly revealed the ionization behavior of the relevant species. The ionizing laser was scanned to obtain a photoionization efficiency (PIE) curve.

**Results and Discussion**

$(DHB)_n$ Clusters

Fig. 1 shows mass spectra obtained by expanding DHB from the heated nozzle under different conditions. For the upper mass spectrum, conditions were adjusted to obtain only smaller clusters, the $(DHB)_n$ n=1 cluster is the largest observed with high intensity. Prominent in the spectrum are ions corresponding to loss of $CO_2$ from DHB. This has been identified from its spectrum as hydroquinone (HQ). HQ is a thermal decomposition product of DHB, and is formed slowly in the nozzle, prior to expansion. It is particularly easily photoionized around 260 nm in a one-color 1 + 1 process (IP= 7.96 eV, (16)). This is the range of ionization wavelengths typically used, and the $HQ^+$ signal at m/z=110 was always strong.

Mixed clusters of DHB and HQ are also apparent, especially $(DHB)_2HQ$. These clusters, both pure DHB or DHB with HQ, were only ionized in a 1 + 1' two-color process. This was verified by blocking the individual lasers and observing that the signals vanished. In the lower spectrum, mixed clusters are very prominent, for two reasons. First the nozzle temperature was somewhat higher, 180¡C vs. 170¡C. This raises the rate of decomposition. Second, the expansion conditions were adjusted for strong cluster formation. As shown by the connecting bars, mixed clusters of DHB with 1-5 HQ molecules are numerous under such conditions.

The 1 + 1' photoionization efficiency curves obtained for $(DHB)_n$ with n up to 10 are shown in Figure 2. As shown previously, strong signal is found for DHB at the vibrationless ionization threshold.(10) This indicates similar geometries in $S_1$ and ion state, and allows direct determination of the adiabatic ionization potential (IP). In contrast, all clusters exhibit severely broadened thresholds, with very gradual approaches to the IP. This makes it necessary to fit the PIE curves in order to estimate the IPs. Up to quartic polynomials were used for this purpose:

$$Z=(h\nu_1 + h\nu_2) - IP$$

$$\text{Ion Signal} \quad = 0, \text{ for } Z < 0 \qquad \text{Eq. 1}$$

$$= \sum_{i=1,4} a_i Z^i, \text{ for } Z \geq 0$$

The degree of the polynomial was chosen to be as small as possible for a good fit. The results of the fits are presented in Table 1.

Such broad, diffuse PIE curves are indicative of large geometry and/or force constant changes between the intermediate excited state and the ion state. The weak signal at

the photoionization threshold is due to poor Franck Condon factors. When distortions of this type are present for multiple normal coordinates, very broad curves like those in Fig. 2 are typical. If only one or a few normal coordinates are distorted, then the PIE curve can take on a stepped shape. This reflects excitations to increasingly higher vibrational levels in the displaced coordinate, in the ion state. In such cases, the location of the first step is often the best measure of the photoionization threshold.

For the $(DHB)_4$ and $(DHB)_5$ clusters weak step structure of this type was found, as shown in Fig. 3. IP estimates from the lowest steps for these clusters are also listed in Table 1. Because the steps are so small, the polynomial fits gave essentially identical IP estimates, but the steps are believed to be more accurate than the fits.

$\underline{(DHB)_n(HQ)_m}$ Clusters

The photoionization thresholds of some mixed DHB-hydroquinone clusters were found to be in the same range as those of the DHB clusters. Figure 4 shows some $(DHB)_n(HQ)_m$ PIE curves, the estimated IPs are listed in Table 2. The IP of free HQ is 7.96 eV,(16) below that of DHB. The larger clusters tend to have slightly lower thresholds than the corresponding $(DHB)_n$ clusters. Most remarkable are the pronounced PIE structure and low threshold of the 1:1 cluster. This is the lowest photoionization threshold of all the clusters studied here. The 1:1 IP may be even lower than shown in Fig. 4, the lower end of the scan was limited by the laser. The structure in the PIE curve is reproducible, and reflects Franck-Condon active modes in the ion state. There are progressions with spacings of 440 and 33 wavenumbers. Further studies of this cluster are clearly necessary.

MALDI Fragmentation and Protonation Reactions

The positive ion MALDI mass spectrum of DHB exhibits strong signals at m/z=137 and 155, in addition to the molecular radical cation at m/z=154. The former corresponds formally to loss of OH, the latter is protonated DHB. The origin of the m/z=137 fragment has been unclear, as is its possible role in MALDI ionization. This ion is not observed in the molecular beam mass spectrum of DHB clusters, nor is protonated DHB. However, m/z=136 is observed in small amounts, about 2 percent of the DHB radical cation signal.

The ion signal at m/z=136 was measured during a scan of the DHB monomer IP region, and is compared with that of the DHB radical cation in Fig. 5. When plotted with the appropriate scale factor, it is readily apparent that the m/z=136 ion first appears at the same two-photon energy as $DHB^+$, and that the shape of the PIE curve is the same. The probability that this is coincidence is very small. Much more probable is that m/z=136 is a prompt fragmentation product of the $DHB^+$ radical cation. Since it appears at the same threshold as DHB ions, but with low yield, the activation energy for fragmentation must be within the upper range of the thermal energies of the cold clusters, or perhaps 100 $cm^{-1}$.

In a warm MALDI plume the yield should increase, but m/z=137 is observed, not 136. This suggests two possibilities: The m/z=136 fragment may form efficiently in the plume from $DHB^+$, but it has a high proton affinity, and reacts quantitatively with neutral DHB to yield m/z=137 and deprotonated DHB. Another possibility is that $(DHB)H^+$ is formed first, perhaps via a proton disproportionation,(4,17) and this ion readily eliminates water to yield m/z=137. The latter route seems more likely since the leaving group is more favorable. This is also supported by the fact that both m/z=136 and 155 ($(DHB)H^+$) are abundant in the MALDI plume, but not in the molecular beam mass spectrum. Both routes are secondary reactions that follow the formation of primary ions. Since $DHB^+$ and $(DHB)H^+$ may be interconvertible via plume collisions,(4) these pathways will not be easy to distinguish.

Implications for MALDI

The cluster size dependence of the photoionization thresholds is shown in Figure 6. Both the polynomial fit results and the estimates from the first step in the curves are shown for tetramer and pentamer. The curve quickly flattens with increasing cluster size. The exponential fit to the data has an asymptotic value of 7.82 eV, which can be taken as a first estimate of the bulk DHB ionization potential. This remains well above the energy of two 337 nm nitrogen laser photons (7.36 eV). Also, the measured ionization efficiency is low until 0.2 eV or more above the apparent IP, as seen in Fig. 2. These facts argue strongly against the simple two-photon model of MALDI ionization, for DHB matrix.

The reduced cluster IPs may nevertheless enhance MALDI ion yield. DHB matrix cluster ions are quite weak in MALDI mass spectra, but there is experimental and theoretical evidence for their existence during the early part of the plume expansion. (13,14) Should these participate in a combined energy pooling/photo-thermal

ionization mechanism, the lower IPs would significantly increase ion yield.(10) In that model the energy gap from a doubly excited state to the ion is bridged by thermal internal energy. The probability of this depends exponentially on the energy gap,(10,18) so a moderately lowered IP can have a significant effect on yield. On the other hand, at high laser fluences, direct multiphoton ionization or pooling processes become more efficient than the thermally assisted process.

Both these regimes are visible in Fig. 7, which shows the calculated ion yield for clusters with an IP of 7.82 eV vs. the free DHB molecule with an IP of 8.0475 eV. The model of Ref. (10) is used, for a 355 nm, 5 ns pulse, and a condensed-phase excited state lifetime of 0.6 ns. Up to about 40 $mJ/cm^2$ the thermal mechanism dominates the ion production, so the reduced cluster IP has a large effect. The yield increases as the fluence, and hence the peak temperature, increases. Above 40 $mJ/cm^2$, non-thermal processes are more important because the excitation density becomes quite high.

**Conclusions**

The photoionization efficiency curves of pure DHB and mixed DHB/HQ clusters were measured in a molecular beam. Clusters of up to 10 molecules were successfully studied. The photoionization thresholds were estimated from these curves, and found to rapidly converge to a limit of 7.82 eV for pure DHB clusters. The ionization efficiency was also found to rise only slowly above the thresholds.

Mixed clusters of DHB with hydroquinone were generally similar, with typical estimated IPs that are slightly less than those of the corresponding DHB clusters. The exception is the 1:1 cluster, which has the lowest IP of all the clusters measured, and a highly structured PIE curve.

These data argue strongly against a simple 2-photon ionization model for primary ionization with this matrix. However, the reduced IPs of the clusters may be important for more complex mechanisms, as demonstrated for the energy pooling/photo-thermal model.

An ion-state fragmentation product of DHB was observed at m/z=136. The abundant m/z=137 ion observed in the DHB MALDI mass spectrum is proposed to be the protonated form of this molecule, and to form in an analogous reaction from $(DHB)H^+$.

**Literature Cited**

1. M. Karas, D. Bachmann and F. Hillenkamp, *Anal. Chem.* **57,** 2935 (1985).

2. *Mass Spectrometry in Biomolecular Sciences*; R. M. Caprioli, A. Malorni and G. Sidona, Eds.; Kluwer: Dordrecht, The Netherlands, (1996)

3. *Protein and Peptide Analysis by Mass Spectrometry*; J. R. Chapman, Ed.; Humana Press: Totowa, NJ, (1996)

4. R. Knochenmuss, A. Stortelder, K. Breuker and R. Zenobi, *J. Mass Spectrom.* **35,** 1237 (2000).

5. R. Zenobi and R. Knochenmuss, *Mass Spectrom. Rev.* **17,** 337 (1998).

6. R. Knochenmuss, E. Lehmann and R. Zenobi, *Eur. Mass Spectrom.* **4,** 421 (1998).

7. H. Ehring, M. Karas and F. Hillenkamp, *Org. Mass Spectrom.* **27,** 427 (1992).

8. P.-C. Liao and J. Allison, *J. Mass Spectrom.* **30,** 408 (1995).

9. M. Karas, M. Glückmann and J. Schäfer, *J. Mass Spectrom.* **35,** 1 (2000).

10. V. Karbach and R. Knochenmuss, *Rapid Commun. Mass Spectrom.* **12,** 968 (1998).

11. R. Cramer, R. F. Haglund Jr. and F. Hillenkamp, *Int. J. Mass Spectrom. Ion Proc.* **169/170,** 51 (1997).

12. A. A. Puretzky and D. B. Geohegan, *Chem. Phys. Lett.* **286,** 425 (1997).

13. M. Handschuh, S. Nettesheim and R. Zenobi, *Appl. Surf. Sci.* **137,** 125 (1998).

14. L. V. Zhigilei and B. J. Garrison, *Appl. Phys. A* **69,** S75 (1999).

15. R. Knochenmuss and A. Vertes, *J. Phys. Chem. B* **104,** 5406 (2000).

16. S. G. Lias, H. M. Rosenstock, K. Draxl, B. W. Steiner, J. T. Herron, J. L. Holmes, R. D. Levin, J. F. Liebman and S. A. Kafafi, *Ionization Energetics Data*. In *NIST Standard Reference Database No. 69*; Mallard, W. G., Ed.; National Institute of Standards and Technology: Gaithersburg, MD 20899 (http://webbok.nist.gov), (1998).

17. K. Breuker, R. Knochenmuss and R. Zenobi, *Int. J. Mass Spectrom.* **184,** 25 (1999).

18. D. A. Allwood, P. E. Dyer and R. W. Dreyfus, *Rapid Commun. Mass Spectrom.* **11,** 499 (1997).

Table 1. Photoionization thresholds of $(DHB)_n$ clusters from the data in Figure 2. The thresholds are estimated from fits to Eqn. 1, and/or from the lowest step found in the PIE curve.

| Size | IP Fit (eV) | lowest step |
|---|---|---|
| 1 | | $8.0475 \pm 0.0005$ |
| 2 | $7.94 \pm 0.02$ | |
| 3 | $7.85 \pm 0.03$ | |
| 4 | $7.80 \pm 0.02$ | $7.85 \pm 0.01$ |
| 5 | $7.81 \pm 0.02$ | $7.84 \pm 0.01$ |
| 6 | $7.83 \pm 0.02$ | |
| 7 | $7.81 \pm 0.04$ | |
| 8 | $7.84 \pm 0.02$ | |
| 10 | $7.82 \pm 0.02$ | |

Table 2. Photoionization thresholds of $(DHB)_n(HQ)m$ clusters from the data in Figure 4, in eV. The thresholds are estimated from fits, and/or from the lowest vibrational structure found in the PIE curve.

| Size (n/m) | IP Fit (eV) | Lowest structure (eV) |
|---|---|---|
| 1:1 | | ≤7.72 |
| 2:1 | 7.82 (+0.02, −0.03) | |
| 3:1 | 7.85 ± 0.03 | |
| 4:1 | 7.78 (+0.02, −0.03) | |
| 5:1 | 7.70 (+0.02, −0.03) | |

**Figures**

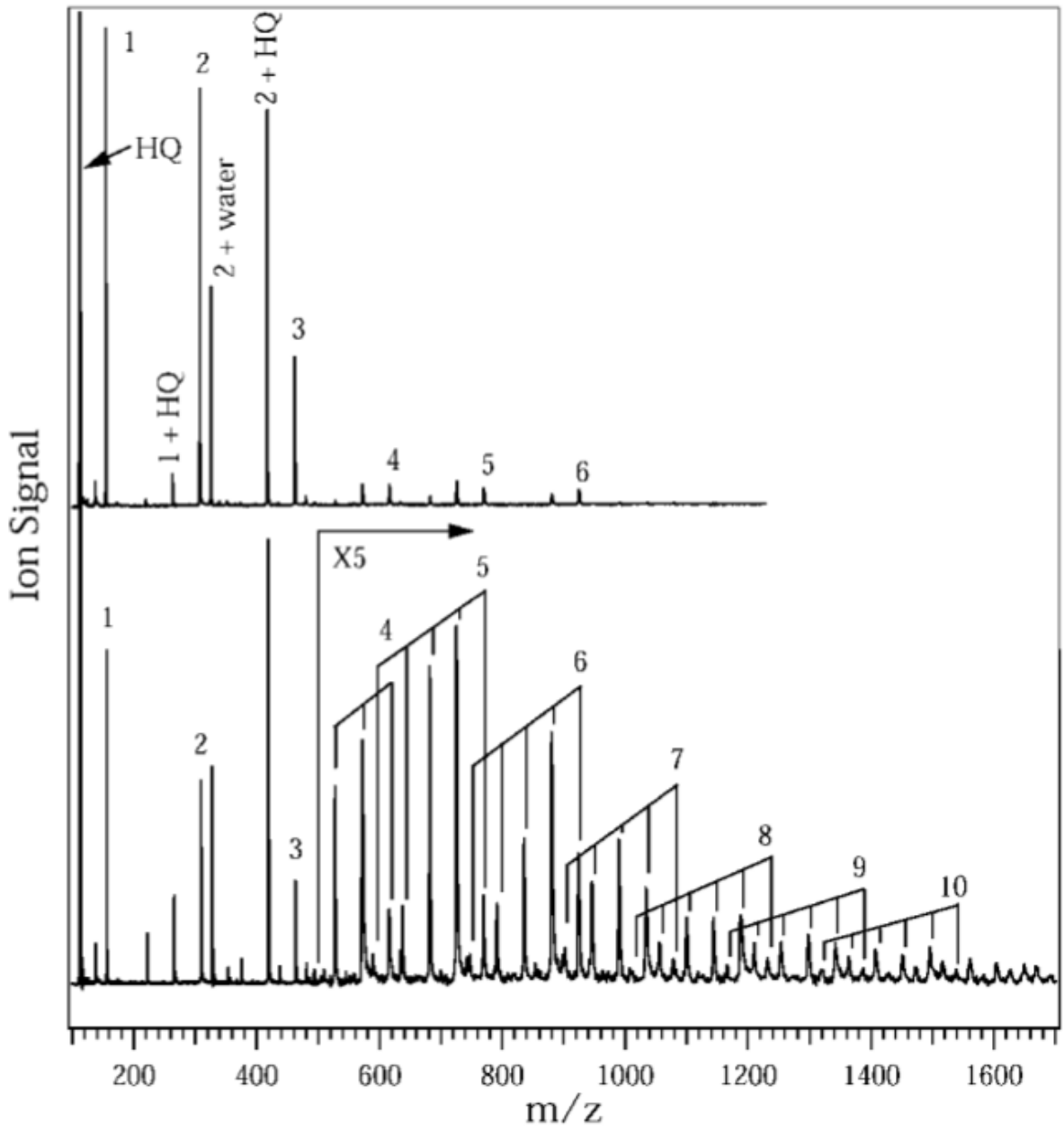


Figure 1. Resonant 2-photon ionization mass spectra of DHB (MW=154 Da) and mixed DHB/HQ (MW of HQ=110 Da) clusters, under two different molecular beam expansion conditions. In the top spectrum the conditions were adjusted to yield small to medium cluster sizes. In the lower spectrum larger clusters were generated, including many mixed clusters. The numbers indicate the sizes of pure $(DHB)_n$ clusters. The raster patterns indicate clusters with the same total number of molecules, but with increasing HQ content: $(DHB)_{n-m}(HQ)_m$.

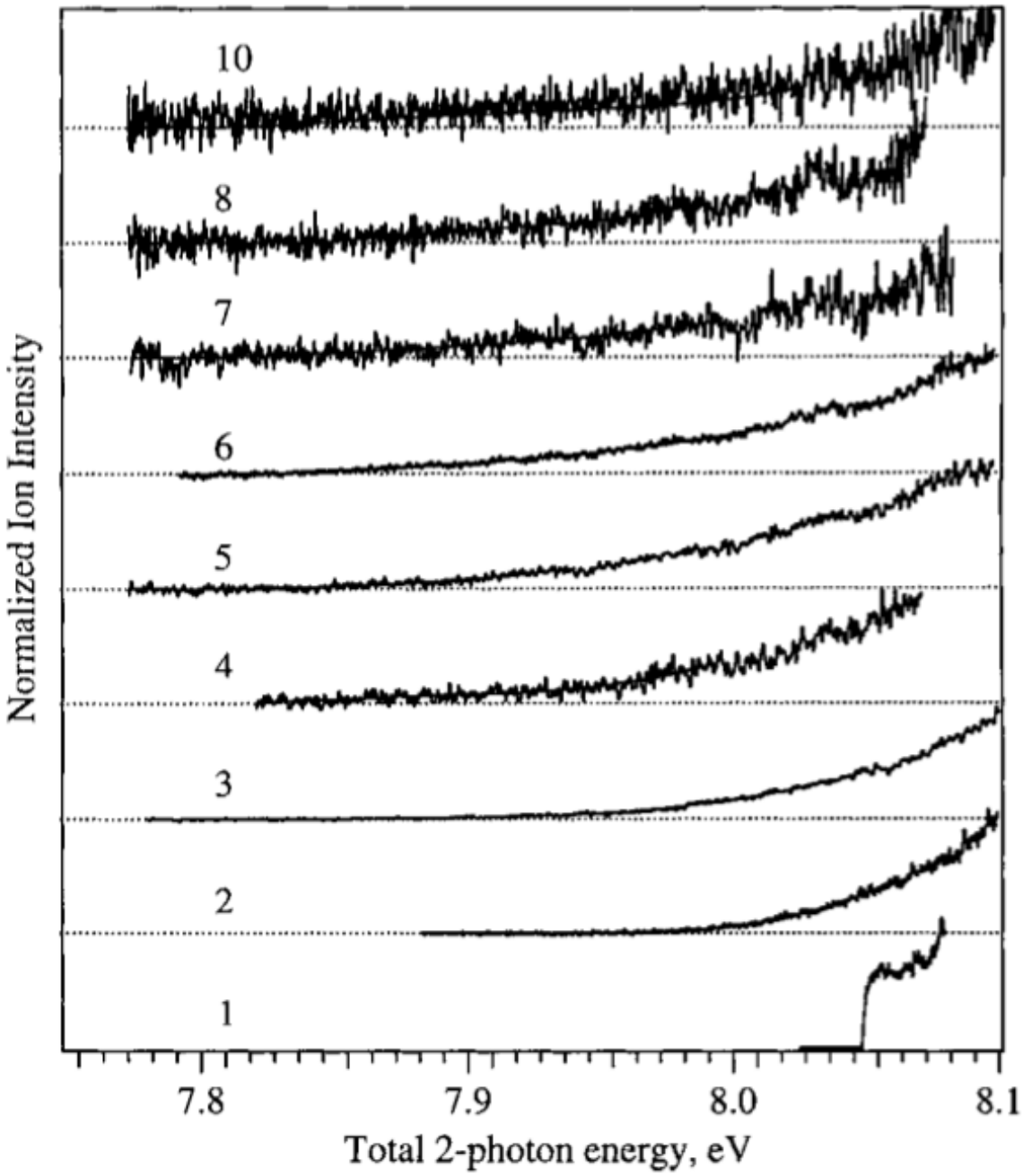


Figure 2. Two-color photoionization efficiency curves of $(DHB)_n$ clusters up to n=10. The excitation wavelengths were optimized for each cluster, and were typically in the range of 361.5 - 362.5 nm.

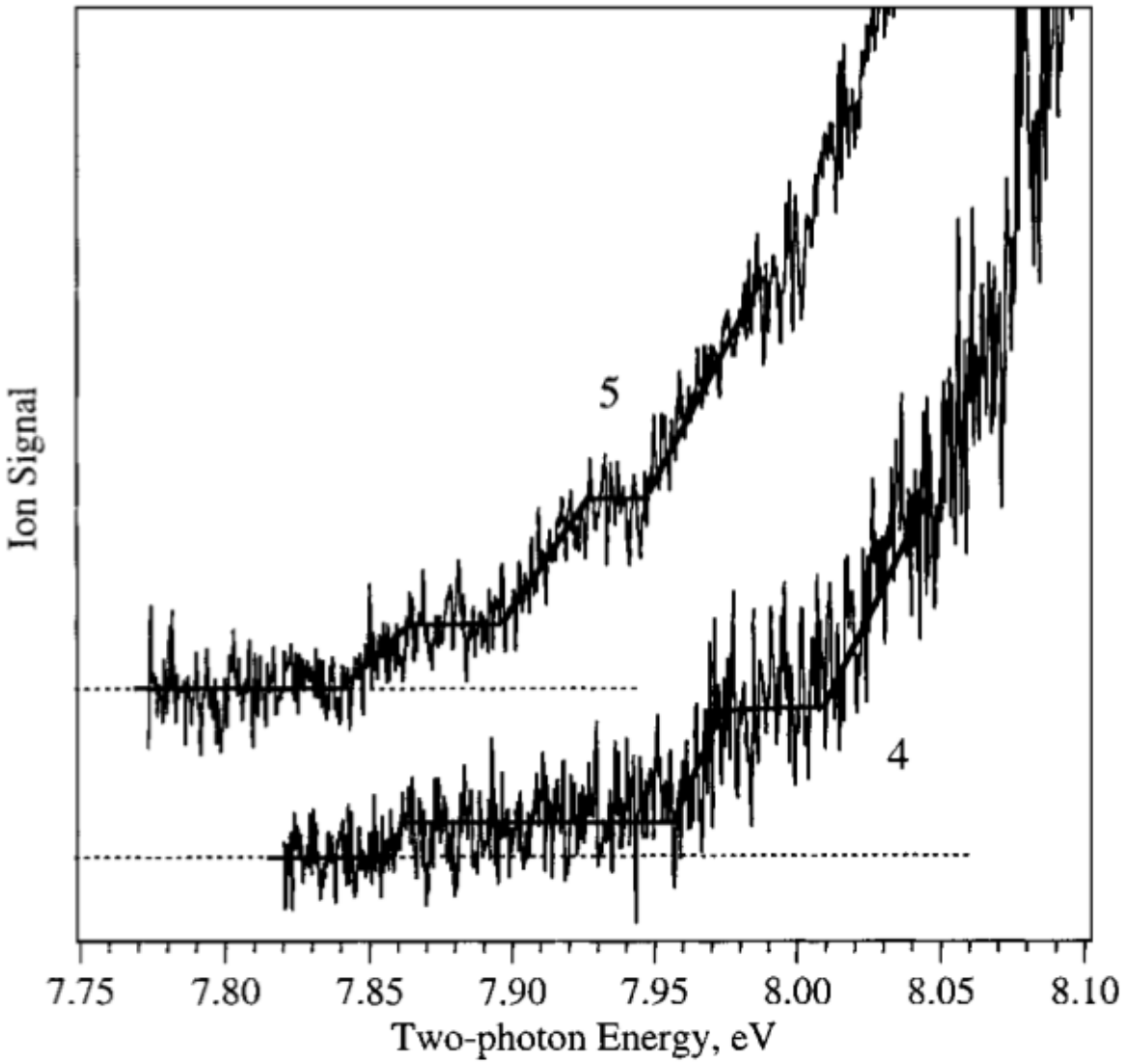


Figure 3. Two-color photoionization efficiency curves for $(DHB)_{n=4,5}$ clusters. The vibrational steps in the curves are indicated by the solid lines.

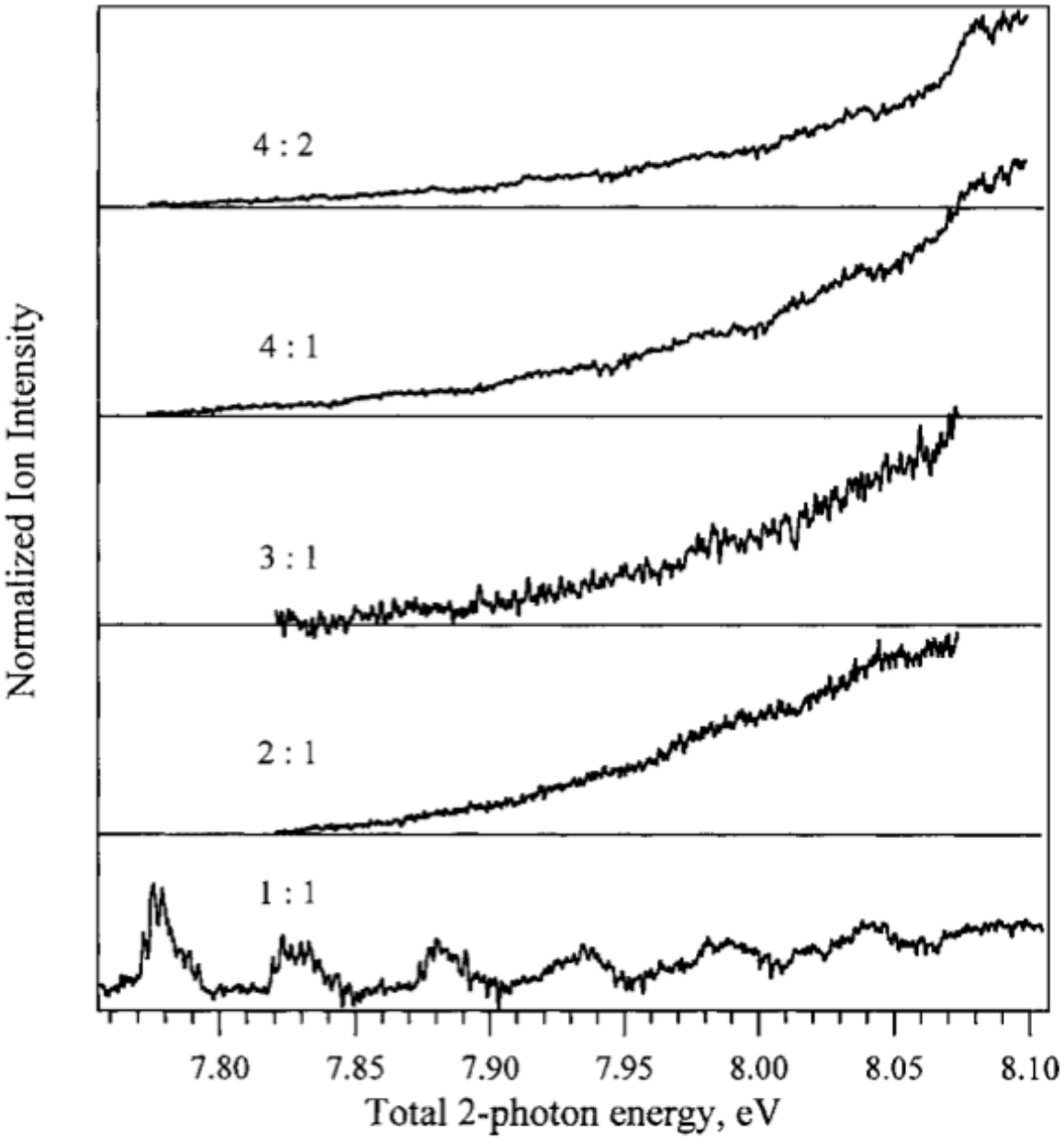


Figure 4. Two-color photoionization efficiency curves for $(DHB)_n(HQ)_m$ mixed clusters. The cluster composition is indicated as n:m.

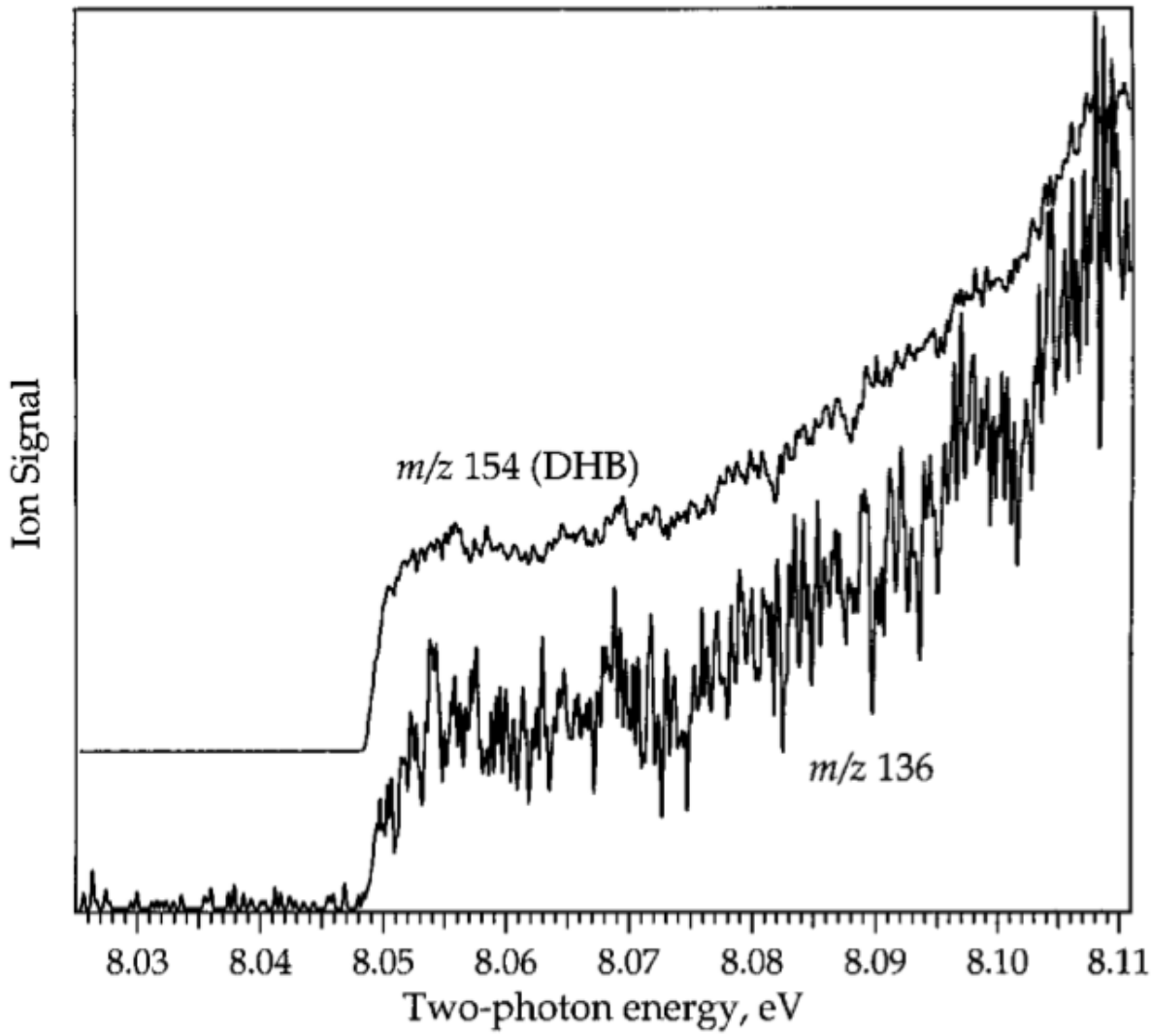


Figure 5. Two-color photoionization efficiency curves for DHB monomer and the ion appearing at m/z=136. The latter is scaled for comparison with the DHB curve. Excitation was at 357.58 nm, on an absorption band of DHB.

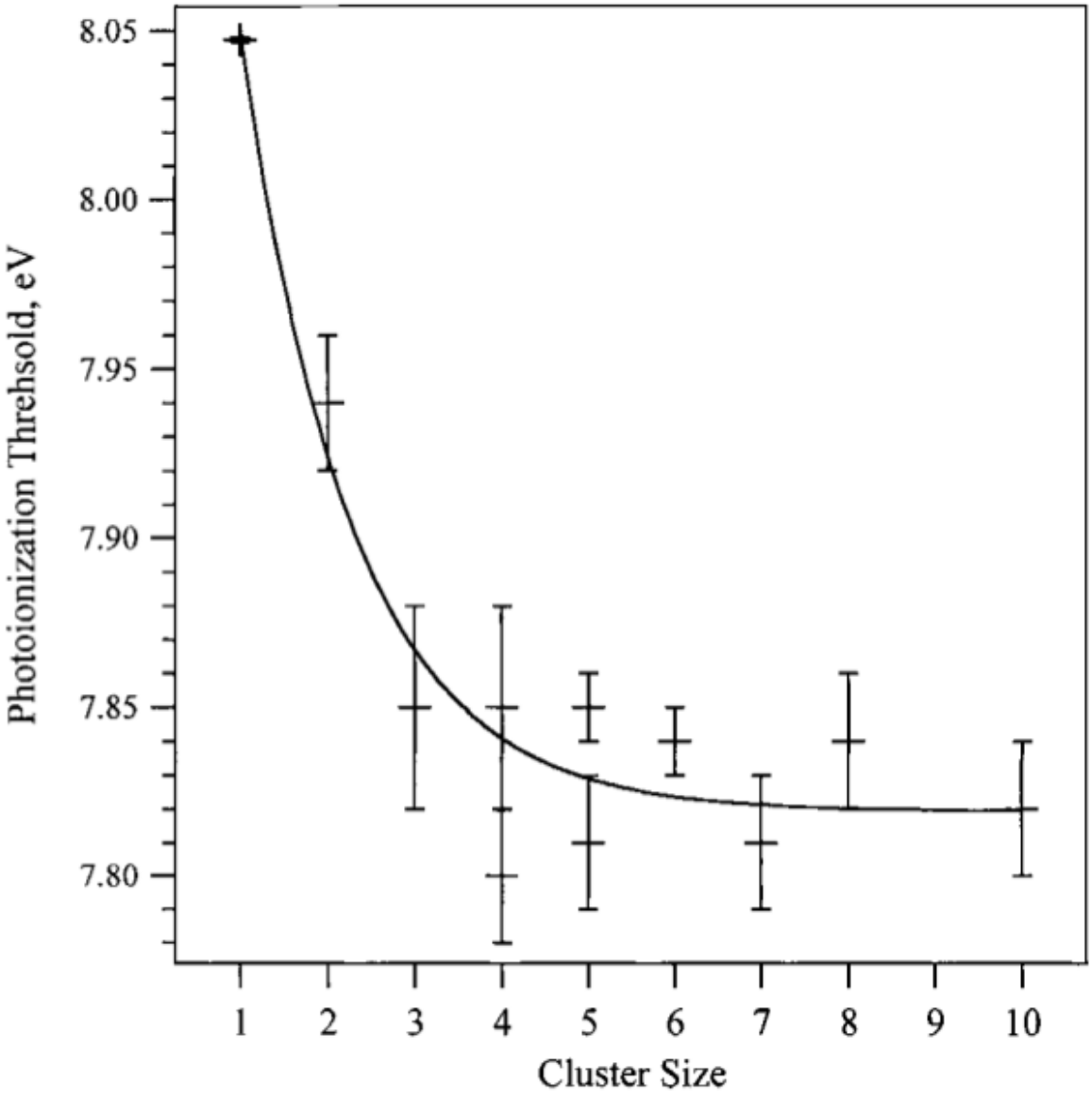


Figure 6. Measured 2-photon ionization thresholds for DHB clusters as a function of cluster size. See also Table 1. The exponential fit reaches an asymptotic value of 7.82 eV at large sizes.

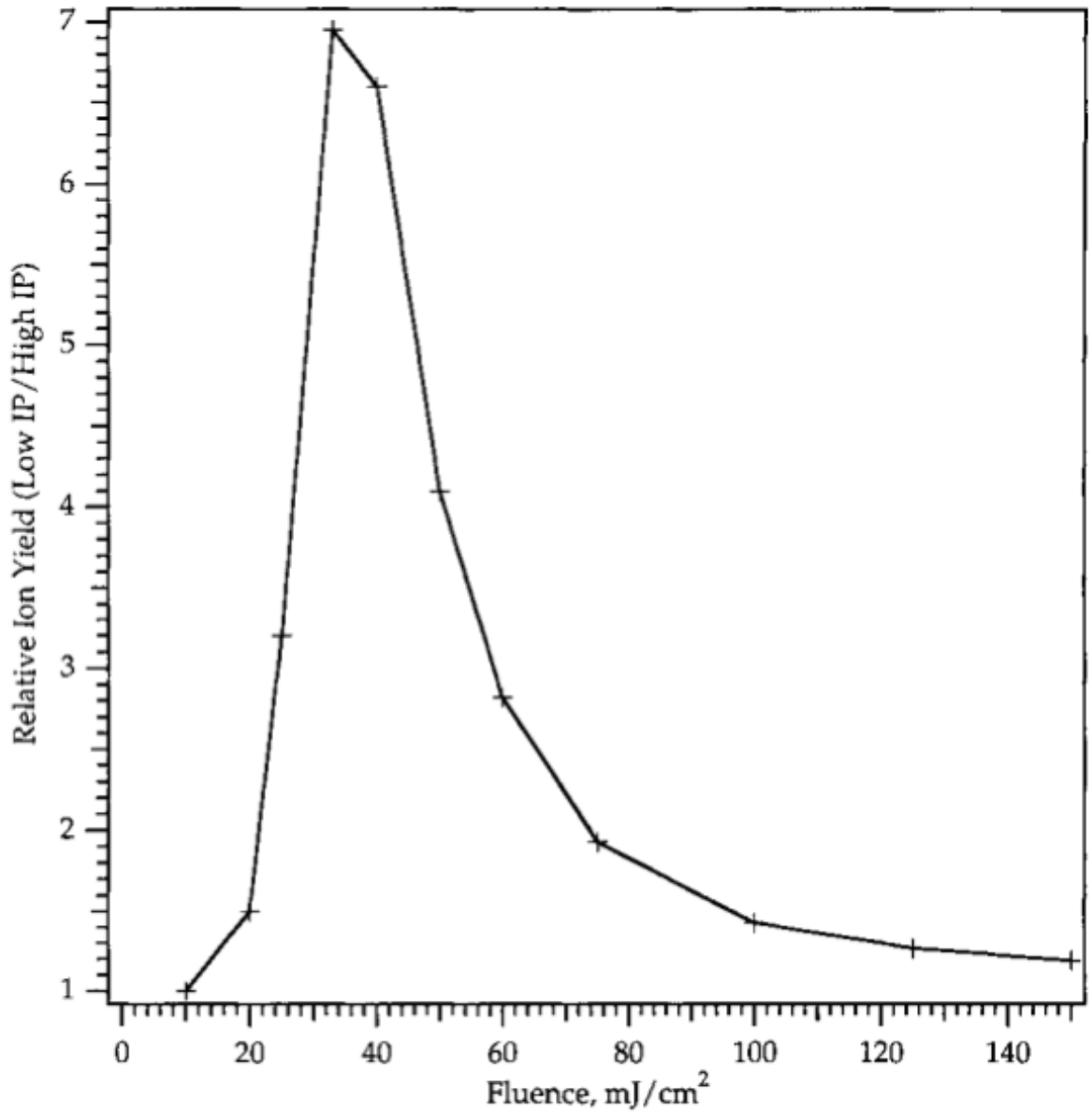


Figure 7. Calculated relative ion yields for low-IP (7.82 eV) DHB clusters vs. high-IP (8.0475 eV) DHB monomer, as a function of laser fluence. The model is that of Ref. (10), for a 355 nm, 5 ns laser pulse, and a 0.6 ns excited state lifetime.